J. Fluid Mech. (2001), *vol.* 446, *pp.* 173–198. © 2001 Cambridge University Press
DOI: 10.1017/S0022112001005730 Printed in the United Kingdom

Eddy viscosity of cellular flows

By ALEXEI NOVIKOV[1] AND GEORGE PAPANICOLAOU[2]

[1]IMA, University of Minnesota, 400 Lind, 207 Church S.E., Minneapolis, MN 55455, USA
e-mail: novikov@ima.umn.edu

[2]Department of Mathematics, Stanford University, Stanford, CA 94305-2125, USA
e-mail: papanico@math.stanford.edu

(Received 17 April 2000 and in revised form 15 May 2001)

We analyse modulational (large-scale) perturbations of stationary solutions of the two-dimensional incompressible Navier–Stokes equations. The stationary solutions are cellular flows with stream function $\phi = \sin y_1 \sin y_2 + \delta \cos y_1 \cos y_2$, $0 \leqslant \delta \leqslant 1$. Using multiscale techniques we derive effective coefficients, including the eddy viscosity tensor, for the (averaged) modulation equations. For cellular flows with closed streamlines we give rigorous asymptotic bounds at high Reynolds number for the tensor of eddy viscosity by means of saddle-point variational principles. These results allow us to compare the linear and nonlinear modulational stability of cellular flows with no channels and of shear flows at high Reynolds number. We find that the geometry of the underlying cellular flows plays an important role in the stability of the modulational perturbations. The predictions of the multiscale analysis are compared with direct numerical simulations.

1. Introduction and formulation

One of the basic questions in the study of effective equations for fluids at high Reynolds number concerns the structure of the Reynolds stress tensor, which is responsible for the interaction between small-scale eddies and large-scale flows (see Mohammadi & Pironneau 1994). Our goal in this paper is to derive homogenized or large-scale equations in which the Reynolds stress tensor comes from multiscale analysis, and to analyse how the small-scale eddies determine the effective coefficients of the large-scale equations at high Reynolds number. We model the small-scale eddies by stationary periodic solutions of the two-dimensional incompressible Navier–Stokes equations and the large-scale flow as an initial modulational perturbation of these solutions.

The evolution of the large-scale, modulational, perturbations determines the nonlinear stability of the small-scale cellular flows. We show in this paper that they are unstable at large Reynolds numbers and we determine in detail the dependence of the instability on the anisotropy of the small-scale flows. The modulational stability of shear and cellular flows has been studied by multiscale homogenization methods in the past by many authors: Dubrulle & Frisch (1991); Frisch, She & Sulem (1987); Gama, Vergassola & Frisch (1994); Meshalkin & Sinai (1961); Nepomnyashchy (1976); Sivashinsky (1985); Sivashinsky & Frenkel (1992); Sivashinsky & Yakhot (1985); Wirth, Gama & Frisch (1995). The analysis of cellular flows is restricted, however, to small Reynolds numbers. In this paper we present a stability analysis of shear and cellular flows at high Reynolds numbers. The applicability of modulational

https://doi.org/10.1017/S0022112001005730 Published online by Cambridge University Press

stability studies is considerably enhanced, for example in geophysical modelling, by our large Reynolds number analysis of cellular flows.

Let $\boldsymbol{U}(\tau, y)$ satisfy the two-dimensional incompressible Navier–Stokes equations driven by a spatially periodic force $\boldsymbol{F}(y)$,

$$\partial_\tau \boldsymbol{U}(\tau, y) + \boldsymbol{U}(\tau, y) \cdot \partial \boldsymbol{U}(\tau, y) = -\partial \tilde{P}(\tau, y) + \frac{1}{Re}\Delta \boldsymbol{U}(\tau, y) + \boldsymbol{F}(y), \tag{1.1}$$

$$\partial \cdot \boldsymbol{U}(\tau, y) = 0.$$

Here the Reynolds number,

$$Re = \frac{UL}{\nu},$$

is based on the length scale L, which is proportional to the spatial period of the force, taken to be equal to 2π. The stream function $\Phi(\tau, y)$, such that

$$\boldsymbol{U}(\tau, y) = \begin{pmatrix} -\partial_2 \Phi(\tau, y) \\ \partial_1 \Phi(\tau, y) \end{pmatrix}$$

satisfies the two-dimensional incompressible Navier–Stokes equations in vorticity form:

$$\partial_\tau \Delta\Phi(\tau, y) + J_{yy}(\Phi(\tau, y), \Delta\Phi(\tau, y)) = \frac{1}{Re}\Delta\Delta\Phi(\tau, y) + f(y), \tag{1.2}$$

where for any u and v

$$J_{yy}(u, v) = -\partial_2 u \partial_1 v + \partial_1 u \partial_2 v.$$

Here $f(y) = -\partial_2 F_1(y) + \partial_1 F_2(y)$ is 2π periodic on R^2. It is chosen so that it gives rise to a stream function $\phi(y)$ which is a time-independent, mean-zero, periodic solution of the incompressible Navier–Stokes equations

$$J_{yy}(\phi(y), \Delta\phi(y)) = \frac{1}{Re}\Delta\Delta\phi(y) + f(y). \tag{1.3}$$

Let

$$\Phi(\tau, y) = \phi(y) + \tilde{\Phi}(\tau, y)$$

be a perturbation of the stationary solution $\phi(y)$. If the stream function of the basic flow is an *eddy* of size $\kappa^{-1/2}$, that is if $\phi(y)$ is an eigenfunction of the Laplacian

$$\Delta\phi = -\kappa\phi, \tag{1.4}$$

then the driving force $f(y)$ is

$$f(y) = -\frac{\kappa^2}{Re}\phi(y)$$

and $\tilde{\Phi}(\tau, y)$ satisfies

$$\partial_\tau \Delta\tilde{\Phi}(\tau, y) + J_{yy}(\phi(y), (\kappa + \Delta)\tilde{\Phi}(\tau, y)) + J_{yy}(\tilde{\Phi}(\tau, y), \Delta\tilde{\Phi}(\tau, y)) = \frac{1}{Re}\Delta\Delta\tilde{\Phi}(\tau, y). \tag{1.5}$$

What concerns us here is the stability of eddy flows like (1.3) and (1.4) subject to an initial *modulational* perturbation, a perturbation on a scale much larger than that of the eddy. For this purpose, we introduce a small parameter ϵ and define large-scale time and space variables

$$t = \epsilon^2 \tau, \quad x = \epsilon y \tag{1.6}$$

https://doi.org/10.1017/S0022112001005730 Published online by Cambridge University Press

respectively, and analyse a special class of asymptotic solutions of (1.5), where $\tilde{\Phi}(\tau, y) = \Psi^\epsilon(t, x)$ is expressed in the large-scale or slow variables as

$$\Psi^\epsilon(t,x) = \Psi(t,x) + \epsilon\Psi^1(t,x,x/\epsilon) + \epsilon^2\Psi^2(t,x,x/\epsilon) + \cdots. \tag{1.7}$$

The stream function of the full flow is

$$\phi(x/\epsilon) + \Psi(t,x) + \epsilon\Psi^1(t,x,x/\epsilon) + \cdots. \tag{1.8}$$

The assumption for the dependence on the small-scale or fast spatial variable $y = x/\epsilon$ is that $\Psi^1(t,x,y), \Psi^2(t,x,y), \ldots$ are periodic in the last variable with zero average over a period *cell*, which we denote by $\square = [0, 2\pi\epsilon] \times [0, 2\pi\epsilon]$:

$$\langle \Psi^1(t,x,\cdot)\rangle = 0, \quad \langle \Psi^2(t,x,\cdot)\rangle = 0, \ldots.$$

For any function $u(x,y)$ periodic in the last variable, the *cell-average* $\langle u\rangle(x) = \langle u(x,\cdot)\rangle$ is defined by

$$\langle u\rangle(x) = \frac{1}{\text{Volume}(\square)} \int_\square u(x,y)\,\mathrm{d}y. \tag{1.9}$$

The functions $\Psi^1(t,x,y), \Psi^2(t,x,y), \ldots$ are determined by the zeroth-order modulational stream function $\Psi(t,x)$ and the small-scale stream function $\phi(y)$. This dependence is determined by the multiscale expansion. The initial conditions

$$\Psi^\epsilon(t,x)|_{t=0} = \Psi(x) + \epsilon\Psi^1(x,y) + \epsilon^2\Psi^2(x,y) + \cdots \tag{1.10}$$

are supported in $x \in \Omega$, and $\Psi(x)$ is bounded and smooth, with $\Psi^1(x,y), \Psi^2(x,y), \ldots$ compatible with the expansion (1.7).

Problems of this kind arise when modelling averaged large-scale flows in the presence of small-scale flows. An example is large-scale circulation in the oceans. One of the characteristic features of fluid dynamics in the oceans is the presence of cell-like mesoscale flows on the scale of order 10^4–10^5 m, and velocity fields on larger scales $\approx 10^6$ m (see Cushman-Roisin 1994). If the large-scale flow is regarded as a homogeneous fluid with dynamical properties different from the original, then the effective coefficients of the large-scale modulation equations need to be determined by separation of scales asymptotics. One of these coefficients, the eddy viscosity, is a four-tensor that relates the large-scale deviatoric stress to the large-scale rate of strain.

The concept of eddy viscosity is widely used in the geophysics of the oceans (see Starr 1968; Kraichnan 1976; Monin & Ozmidov 1985) and in astrophysics (see Rüdiger 1989) to treat phenomena of depleted, in some cases even 'negative' diffusion, that accompany transport of vector quantities. This is different from the transport of scalar quantities, which is truly diffusive. The presence of micro-structure in the latter case only enhances diffusion.

Various examples of flows with large-scale instabilities arising from negative eddy viscosity have been discussed in the literature. The most well studied among them is the Kolmogorov flow, a special case of a two-dimensional time-independent periodic shear flow (see Meshalkin & Sinai 1961; Nepomnyashchy 1976; Sivashinsky 1985; Dubrulle & Frisch 1991). The one-dimensional nature of this problem allows detailed analysis of various types of instabilities including nonlinear effects.

Fully two- and three-dimensional flows are analysed mostly numerically, or by using asymptotic expansions for small Reynolds number, because of their analytical complexity. Reductions and simplifications can be achieved for problems with a non-trivial group of symmetries. Parity-invariance, i.e. the presence of a centre of spatial

https://doi.org/10.1017/S0022112001005730 Published online by Cambridge University Press

symmetry, is recognized (see Kraichnan 1976; Dubrulle & Frisch 1991 and references therein) as a sufficient condition for eddy-viscous dynamics. Some two-dimensional flows (analysed in Sivashinsky & Yakhot 1985; Sivashinsky & Frenkel 1992; Gama *et al.* 1994) possess this important property. Nevertheless, the mathematical theory of eddy viscosity is restricted to small Reynolds numbers (see Dubrulle & Frisch 1991) and there is not much known, even in the linearized case, for when the Reynolds number is not small.

In § 2 we use multiscale analysis to derive eddy viscosities as effective coefficients for the transport of a large-scale perturbation of stationary small-scale eddies. In § 2.3 we derive from equation (1.5) the large-scale modulation equation for $\Psi(t,x)$ in vorticity form:

$$\partial_t \nabla^2 \Psi(t,x) + \alpha^{nonlin}_{jikl} \nabla_j \nabla_i (\nabla_k \Psi(t,x) \nabla_l \Psi(t,x)) = \nu_{jikl} \nabla_j \nabla_i \nabla_k \nabla_l \Psi(t,x). \tag{1.11}$$

Here we use the summation convention and the notation

$$\nabla_i = \frac{\partial}{\partial x_i}.$$

The coefficients ν_{jikl} are the tensor of eddy viscosity and α^{nonlin}_{jikl} are the effective coefficients of another tensor which we call the *nonlinear α-tensor*. Both tensors are derived as necessary solvability conditions of auxiliary cell problems that guarantee the validity of the separation of scales for some finite time. Modulation equations like (1.11) have been derived before (see e.g. Dubrulle & Frisch 1991) and are presented briefly here for completeness.

In the rest of the paper we consider eddies with $\kappa = 2$, a family of cellular flows with a stream function

$$\phi = \sin y_1 \sin y_2 + \delta \cos y_1 \cos y_2, \quad 0 \leqslant \delta \leqslant 1. \tag{1.12}$$

In § 3 we analyse the tensor of eddy viscosity of cellular flows for large Reynolds numbers. All the coefficients of the eddy viscosity tensor ν_{jikl} but one, called ν', are computed analytically. The ν' is computed numerically for $Re \leqslant 32$, and for closed cellular flows $\phi = \sin y_1 \sin y_2$ we show that $\nu' = O(Re^{2.5})$ for large Re. This large Reynolds number analysis is the main result of this paper.

In § 4 we study the linear and nonlinear stability of the modulational equations. In § 4.1 we compare the linear dispersion relations of the modulational equations for closed cellular flows and for shear flows for large Reynolds number. The modulational perturbations of closed cellular flows ($\delta = 0$ in (1.12)) are much more stable than the shear cellular flows ($\delta = 1$ in (1.12)) for large Reynolds numbers. More specifically, exponential solutions $\Psi(t,x) = \exp(\sigma t)\exp(k_1 x_1 + k_2 x_2)$ are asymptotically unstable as $Re \to \infty$ *only if* $k_1 \approx \pm k_2$ for closed cellular flows (equation (4.5)). This result is to be contrasted with a similar stability result for shear flows, where exponential solutions are asymptotically unstable as $Re \to \infty$ if $C_1 \leqslant |k_1|/|k_2| \leqslant C_2$ (equation (4.6)), where $C_1 = 1/C_2 \approx 0.45 \neq 1$. Our new results here show that because of the presence of $\nu' = O(Re^{2.5})$ for closed cellular flows, the stability at high Reynolds numbers is significantly better for flows with closed streamlines. Cell-like mesoscale ocean flows are at rather high Reynolds number $Re = 10$–10^3 and are close to closed cellular flows (see Cushman-Roisin, McLaughlin & Papanicolaou 1984), so our analysis may provide an explanation for the persistence of these flows. In § 4.2 we present results of numerical experiments which show that the nonlinear modulational equation is stable (unstable) if the linear modulational equation is stable (unstable). In other words, the presence of the nonlinear α-tensor in (1.11) does not affect the

https://doi.org/10.1017/S0022112001005730 Published online by Cambridge University Press

conclusions of the linear stability analysis of Sivashinsky & Yakhot (1985) that we recover for small Reynolds numbers, and this tensor does not affect the conclusions of our linear stability analysis for large Reynolds numbers.

In § 5 we compare the results of the multiscale analysis with direct numerical simulations of the linearized problem (1.5). In the Appendix we show with new variational principles and analysis that for closed cellular flows $v' = O(Re^{2.5})$ for large Reynolds number Re.

2. Multiscale analysis for cellular flows

2.1. *Separation of scales*

Loosely speaking the separation of scales assumption states that the fast and slow scales can be treated as independent, and if the separation of scales is present at $\tau = 0$ then it persists at least for some finite time $T_\epsilon = \epsilon^{-n} T_0$, where the exponent n is chosen appropriately. For the case $\Delta\phi = -\kappa\phi$, $n = 2$.

In the expansion (1.7) we treat x and y as independent variables and replace the time and space derivatives by

$$\partial_i \to \partial_i + \epsilon\nabla_i, \quad \partial_\tau \to \epsilon^2\partial_t, \tag{2.1}$$

where ∇ denotes partial derivatives with respect to the slow spatial variable x. For the Laplacian in the slow variables we shall use the notation $\nabla^2 = \sum \nabla_i^2$.

Equation (1.5) becomes

$$\begin{aligned}\epsilon^2\partial_t(\Delta + 2\epsilon\partial_i\nabla_i + \epsilon^2\nabla^2)\Psi^\epsilon(t,x,y) &= \frac{1}{Re}(\Delta + 2\epsilon\partial_i\nabla_i + \epsilon^2\nabla^2)^2\Psi^\epsilon(t,x,y)\\ &- (J_{yy} + \epsilon J_{yx})(\phi(y), (\kappa + \Delta + 2\epsilon\partial_i\nabla_i + \epsilon^2\nabla^2)\Psi^\epsilon(t,x,y))\\ &- (J_{yy} + \epsilon(J_{yx} + J_{xy}) + \epsilon^2 J_{xx})(\Psi^\epsilon(t,x,y), (\Delta + 2\epsilon\partial_i\nabla_i + \epsilon^2\nabla^2)\Psi^\epsilon(t,x,y)),\end{aligned} \tag{2.2}$$

where for any u and v

$$\begin{aligned}J_{xy}(u,v) &= -\nabla_2 u\partial_1 v + \nabla_1 u\partial_2 v,\\ J_{yx}(u,v) &= -\partial_2 u\nabla_1 v + \partial_1 u\nabla_2 v,\\ J_{xx}(u,v) &= -\nabla_2 u\nabla_1 v + \nabla_1 u\nabla_2 v.\end{aligned}$$

2.2. *Cell problems*

We substitute expansion (1.7) in equation (2.2) and obtain a family of *cell problems*, that is linear, elliptic, periodic boundary value problems in the fast variable y, where by the assumption of wide separation of scales the slow variables are treated as constant parameters.

The zeroth-order cell problem

$$\frac{1}{Re}\Delta\Delta\Psi(t,x) - J_{yy}(\phi, (\kappa + \Delta)\Psi(t,x)) - J_{yy}(\Psi, \Delta\Psi(t,x)) = 0 \tag{2.3}$$

justifies *a posteriori* that $\Psi(t,x)$ can be chosen independent of the fast variable y.

The first-order cell problem is

$$\frac{1}{Re}\Delta\Delta\Psi^1(t,x,y) - J_{yy}(\phi, (\kappa + \Delta)\Psi^1(t,x,y)) = \kappa J_{yx}(\phi, \Psi). \tag{2.4}$$

https://doi.org/10.1017/S0022112001005730 Published online by Cambridge University Press

Equation (2.4) has the solution $\Psi^1 = (Re/\kappa)J_{yx}(\phi, \Psi)$, since

$$(\kappa + \Delta)J_{yx}(\phi, \Psi) = J_{yx}((\kappa + \Delta)\phi, \Psi) = 0.$$

The second-order cell problem is

$$\frac{1}{Re}\Delta\Delta\Psi^2(t,x,y) - J_{yy}(\phi, (\kappa+\Delta)\Psi^2(t,x,y))$$
$$= 2J_{yy}(\phi, \partial_i\nabla_i\Psi^1) - 4\frac{1}{Re}\Delta\partial_i\nabla_i\Psi^1 + J_{xy}(\Psi(t,x), \Delta\Psi^1(t,x,y)). \tag{2.5}$$

It has the solution

$$\Psi^2(t,x,y) = \frac{4Re}{\kappa^2}\partial_i\nabla_i J_{yx}(\phi, \Psi)$$
$$-\frac{Re^2}{\kappa^2}J_{xy}(\Psi, J_{yx}(\phi, \Psi)) - 2\psi(y)(\nabla_2^2 - \nabla_1^2)\Psi(t,x) + 2\tilde{\psi}(y)\nabla_1\nabla_2\Psi(t,x),$$

where $\psi(y)$ and $\tilde{\psi}(y)$ are solutions of the auxiliary cell problems

$$\frac{1}{Re}\Delta\Delta\psi(y) - J_{yy}(\phi, (\kappa+\Delta)\psi(y)) = -\frac{Re}{\kappa}J_{yy}(\phi, \partial_1\partial_2\phi), \tag{2.6}$$

$$\frac{1}{Re}\Delta\Delta\tilde{\psi}(y) - J_{yy}(\phi, (\kappa+\Delta)\tilde{\psi}(y)) = -\frac{Re}{\kappa}J_{yy}(\phi, (\partial_2^2 - \partial_1^2)\phi). \tag{2.7}$$

The first- and second-order cell problems determine $\Psi^1(t,x,y)$ and $\Psi^2(t,x,y)$ in the expansion (1.7). The third-order cell problem determines $\Psi^3(t,x,y)$ in the expansion (1.7), if it is solvable for arbitrary $\Psi(t,x)$. A necessary, and sufficient in some cases, solvability condition for this cell problems is that its cell average is zero. The third-order cell problem is

$$\frac{1}{Re}\Delta\Delta\Psi^3(t,x,y) - J_{yy}(\phi, (\kappa+\Delta)\Psi^3(t,x,y))$$
$$= \partial_t\Delta\Psi^1(t,x,y) - \frac{1}{Re}(4(\partial_i\nabla_i) + 2\nabla^2\Delta)\Psi^1(t,x,y) - \frac{1}{Re}4\Delta\partial_i\nabla_i\Psi^2(t,x,y)$$
$$+ J_{yx}(\phi(y), \nabla^2\Psi(t,x)) + J_{yy}(\phi(y), 2\partial_i\nabla_i\Psi^1(t,x,y))$$
$$+ J_{yx}(\phi(y), (\kappa+\Delta)\Psi^2(t,x,y)) + J_{xy}(\Psi(t,x), 2\partial_i\nabla_i\Psi^1(t,x,y))$$
$$+ J_{xx}(\Psi(t,x), \Delta\Psi^1(t,x,y)) + J_{xx}(\Psi^1(t,x,y), \nabla^2\Psi^1(t,x,y))$$
$$+ J_{yy}(\Psi^1(t,x,y), 2\partial_i\nabla_i\Psi^1(t,x,y))$$
$$+ (J_{yx} + J_{xy})(\Psi^1(t,x,y), \Delta\Psi^1(t,x,y))$$
$$+ J_{xy}(\Psi(t,x), \Delta\Psi^2(t,x,y)) + J_{yy}(\Psi^1(t,x,y), \Delta\Psi^2(t,x,y))$$
$$+ J_{yy}(\Psi^2(t,x,y), \Delta\Psi^1(t,x,y)). \tag{2.8}$$

The solvability condition for this problem is

$$-\langle J_{yx}(\phi, \nabla^2\Psi)\rangle - 2\langle J_{yx}(\phi, \partial_i\nabla_i\Psi^1)\rangle - \langle J_{yx}(\phi, (\kappa+\Delta)\Psi^2)\rangle = 0. \tag{2.9}$$

The first term in (2.9) vanishes, because Ψ is independent of the fast variables. The

https://doi.org/10.1017/S0022112001005730 Published online by Cambridge University Press

third term vanishes, because $(\kappa + \Delta)\phi = 0$. The second term is zero as well:

$$\begin{aligned}\langle J_{yx}(\phi, \partial_i \nabla_i \Psi^1)\rangle &= \frac{Re}{\kappa}\langle J_{yx}(\phi, \partial_i \nabla_i J_{yx}(\phi, \Psi))\rangle \\ &= \left\langle \partial_1 \frac{(\partial_2\phi)^2}{2} \right\rangle (\nabla_1^3\Psi - \nabla_1\nabla_2^2\Psi) + \left\langle \partial_2 \frac{(\partial_1\phi)^2}{2} \right\rangle (\nabla_2^3\Psi - \nabla_1^2\nabla_2\Psi) \\ &\quad + \langle \partial_2(\partial_2^2 - \partial_1^2)\phi\rangle \nabla_1^2\nabla_2\Psi - \langle \partial_1(\partial_2^2 - \partial_1^2)\phi\rangle \nabla_1\nabla_2^2\Psi \\ &= \langle \partial_2((\partial_2\phi)^2 + \tfrac{1}{2}\kappa\phi^2)\rangle \nabla_1^2\nabla_2\Psi + \langle \partial_1((\partial_1\phi)^2 + \tfrac{1}{2}\kappa\phi^2)\rangle \nabla_1^2\nabla_2\Psi = 0.\end{aligned}$$

Therefore, since the solvability condition (2.9) is satisfied, $\Psi^3(t, x, y)$ is well defined. We show in the next section that $\Psi^3(t, x, y)$ plays no role in the computation of the effective coefficients of the large-scale modulation equation. Therefore it suffices to know that $\Psi^3(t, x, y)$ is well defined.

It should be noted that the solvability conditions for the zeroth-, first- and second-order cell problems are always satisfied for any mean-zero stream function $\phi(y)$. In general the third-order cell problem has a non-trivial solvability condition. If it is not satisfied, then the scaling should be chosen to be linear in ϵ in space and time. Then the instabilities of the modulation equation are governed by the linear Anisotropic Kinetic Alpha effect, which is similar to the α-effect in magneto-hydrodynamics (see Moiseev *et al.* 1984; Frisch *et al.* 1987; Sulem *et al.* 1989 and references therein).

The solvability condition for the third-order cell problem is satisfied if $\phi(y)$ is parity invariant, that is $\phi(-y) = \phi(y)$. The condition of parity invariance is sufficient, but certainly not necessary, for quadratic-in-ϵ time scaling. The stream functions ϕ, with $\Delta\phi = -\kappa\phi$, that we consider here are not necessarily parity invariant.

2.3. *Effective coefficients of the large-scale equation*

Since $\Psi^1(x, t, y)$, $\Psi^2(x, t, y)$, $\Psi^3(x, t, y)$ are well-defined in terms of $\Psi(x, t)$ by the first-, second- and third-order cell problems, the solvability condition for the fourth-order cell problem determines $\Psi(x, t)$ as a solution of a differential equation for which the fast variable y is eliminated by averaging. This equation is the large-scale modulation equation for $\Psi(t, x)$. In order to compute its (effective) coefficients it is sufficient to know Ψ^1 and Ψ^2 only. The solvability condition for the fourth-order cell problem is

$$\begin{aligned}\partial_t \nabla^2\Psi(x, t) + J_{xx}(\Psi, \nabla^2\Psi) + 2\langle J_{xy}(\Psi^1, \partial_i\nabla_i\Psi^1) + J_{yx}(\Psi^1, \partial_i\nabla_i\Psi^1)\rangle \\ + \langle J_{yx}(\phi, \nabla^2\Psi^1)\rangle + 2\langle J_{yx}(\phi, \partial_i\nabla_i\Psi^2)\rangle - \frac{1}{Re}\nabla^2\nabla^2\Psi(t, x) = 0 \qquad (2.10)\end{aligned}$$

or, in terms of $\Psi(t, x)$ only

$$\begin{aligned}\partial_t \nabla^2\Psi(x, t) + J_{xx}(\Psi, \nabla^2\Psi) - \frac{2Re^2}{\kappa^2}\langle J_{yx}(\phi, \partial_i\nabla_i J_{xy}(\Psi, J_{yx}(\phi, \Psi)))\rangle \\ + \frac{2Re^2}{\kappa^2}\langle J_{xy}(J_{yx}(\phi, \Psi), \partial_i\nabla_i J_{yx}(\phi, \Psi))\rangle \\ + \frac{2Re^2}{\kappa^2}\langle J_{yx}(J_{yx}(\phi, \Psi), \partial_i\nabla_i J_{yx}(\phi, \Psi))\rangle\end{aligned}$$

https://doi.org/10.1017/S0022112001005730 Published online by Cambridge University Press

$$= \frac{1}{Re}\nabla^2\nabla^2\Psi(t,x) - \frac{8Re}{\kappa^2}\langle J_{yx}(\phi,(\partial_i\nabla_i)^2 J_{yx}(\phi,\Psi))\rangle$$
$$+ v'(\nabla_2^2-\nabla_1^2)^2\Psi + (v''+v''')(\nabla_2^2-\nabla_1^2)\nabla_1\nabla_2\Psi + v''''\nabla_1^2\nabla_2^2\Psi. \qquad (2.11)$$

Here the constants

$$v' = -4\langle\partial_1\partial_2\phi\psi\rangle, \quad v'' = -4\langle(\partial_2^2-\partial_1^2)\phi\psi\rangle,$$
$$v''' = -4\langle\partial_1\partial_2\phi\tilde{\psi}\rangle, \quad v'''' = -4\langle(\partial_2^2-\partial_1^2)\phi\tilde{\psi}\rangle$$

are determined in terms of ψ and $\tilde{\psi}$, the solutions of the auxiliary cell problems (2.6) and (2.7). The effective tensors v_{jikl} and α_{jikl}^{nonlin} for equation (1.11) can be read off from (2.11).

2.4. *Summary of the multiscale expansion*

Using a multiscale asymptotic expansion we obtain a hierarchy of cell problems. Their solvability conditions give the appropriate time scaling and the effective coefficients of the large-scale modulation equations simultaneously, with no additional assumptions. The only property of the stationary small-scale periodic stream function ϕ that we use is $\Delta\phi = -\kappa\phi$. This property simplifies the zeroth- and the first-order cell problems and, more importantly, guarantees quadratic scaling in time at least for some fixed large-scale time T_0 that depends on Re and ϕ. It suffices to consider the expansion (1.7) up to order ϵ^4 because the equations for the large-scale stream function $\Psi(t,x)$ come from the solvability condition of the fourth-order cell problem.

The main difficulty in computing the coefficients of the tensor of eddy viscosity is the behaviour of the solutions of the auxiliary cell problems (2.6) and (2.7). For small Reynolds number they give a correction to the tensor of eddy viscosity of order Re^2. In this case the eddy viscosities can be calculated approximately up to $O(Re^2)$ because there is no need to solve auxiliary cell problems and the nonlinear α-tensor can be disregarded. This was carried out in Sivashinsky & Yakhot (1985).

Two questions arise when $Re \to \infty$. One is how the solutions of the auxiliary cell problems may stabilize or destabilize the large-scale modulation equations. The other is whether the nonlinear correction affects the linear stability analysis of the modulation equation. We shall now discuss these two questions for the family of cellular flows $\phi = \sin y_1 \sin y_2 + \delta\cos y_1\cos y_2$, $0 \leqslant \delta \leqslant 1$.

3. Analysis of the tensor of eddy viscosity of cellular flows

Let the stream function be given by $\phi = \sin y_1 \sin y_2 + \delta\cos y_1\cos y_2$ (see figure 1). Then the large-scale modulation equation (2.11) is

$$\frac{\partial\nabla^2\Psi}{\partial t} + \frac{Re^2}{8}(\nabla_2^2-\nabla_1^2)[\delta((\nabla_1\Psi)^2+(\nabla_2\Psi)^2) + (1+\delta^2)\nabla_1\Psi\nabla_2\Psi] + J_{xx}(\Psi,\nabla^2\Psi)$$
$$= \frac{1}{Re}\nabla^2\nabla^2\Psi - \frac{Re}{8}((\nabla_1+\delta\nabla_2)^2 + (\delta\nabla_1+\nabla_2)^2)\nabla^2\Psi$$
$$+ \left(\frac{Re}{2}(1+\delta^2) + v'\right)(\nabla_2^2-\nabla_1^2)^2\Psi, \qquad (3.1)$$

where the constants v'', v''', and v'''' vanish, since $(\partial_2^2-\partial_1^2)\phi = 0$, and

$$v' = -4\langle\partial_1\partial_2\phi\psi\rangle. \qquad (3.2)$$

https://doi.org/10.1017/S0022112001005730 Published online by Cambridge University Press

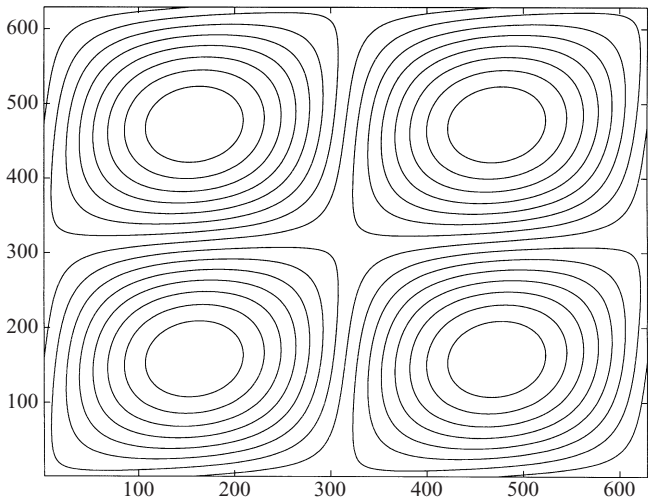


FIGURE 1. Level sets of the stream function of cellular flows with small channels, $\delta = 0.1$.

Here ψ is determined by the cell problem

$$\frac{1}{Re}\Delta\Delta\psi - J_{yy}\left(\phi, (\Delta + 2)\psi - \frac{Re}{2}\partial_1\partial_2\phi\right) = 0. \tag{3.3}$$

The coefficients of the tensor of eddy viscosity can be read off from the right-hand side of equation (3.1). Its analysis boils down to the analysis of the only unknown coefficient v'. We show that v' is always non-negative. We also compute v' numerically for $Re = 1, 2, \ldots, 32$. In the special case of *closed* cellular flows $\phi = \sin y_1 \sin y_2$, we show in the Appendix that $v' = O(Re^{2.5})$, $Re \to \infty$.

3.1. *Numerical values of v' for intermediate Reynolds numbers*

Let ψ be the solution of (3.3). Note that it satisfies

$$\left.\begin{aligned} \psi(y_1 + \pi, y_2 + \pi) &= \psi(y_1, y_2), \\ \psi(-y_1, -y_2) &= \psi(y_1, y_2), \\ \langle\phi\psi\rangle &= 0. \end{aligned}\right\} \tag{3.4}$$

Therefore for any u such that $\Delta u = -u$, we have $\langle u\psi\rangle = 0$ and

$$\langle(\partial\Delta\psi)^2 - 2(\Delta\psi)^2\rangle \geqslant 0. \tag{3.5}$$

Multiplying equation (3.3) by $(2 + \Delta)\psi(y) - \frac{1}{2}Re\partial_1\partial_2\phi$ and integrating by parts we have

$$\left\langle \frac{1}{Re}\Delta\Delta\psi(y)(2 + \Delta)\psi(y) - \frac{Re}{2}\partial_1\partial_2\phi \right\rangle = 0.$$

Therefore

$$v' = -4\langle\psi\partial_1\partial_2\phi\rangle = \frac{2}{Re}(\langle(\partial\Delta\psi)^2 - 2(\Delta\psi)^2\rangle) \geqslant 0.$$

Equality in (3.5) occurs only when $\Delta\psi = -2\psi$, which is a solution of equation (3.3) only when $\delta = 1$.

Thus, v' is always a non-negative number and vanishes only if $\delta = 1$, that is, if

https://doi.org/10.1017/S0022112001005730 Published online by Cambridge University Press

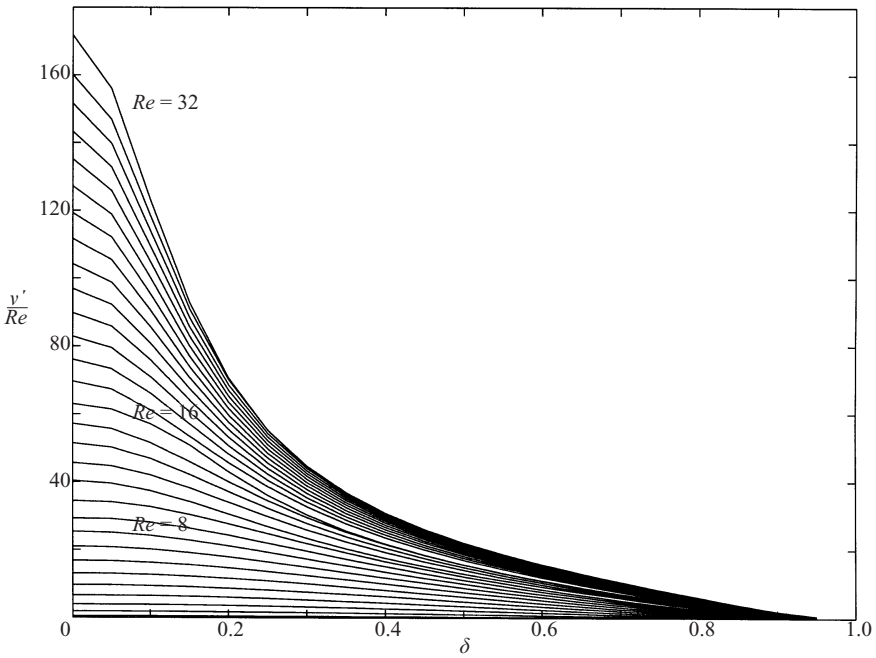


FIGURE 2. Dependence of v'/Re on δ for $Re = 1, 2, \ldots, 32$.

$\phi = \cos(y_1 - y_2)$ is the stream function of a shear flow. This implies that the last term on the right-hand side of equation (3.1) always plays a stabilizing role.

For intermediate Reynolds numbers the dependence of v' on Re and δ is shown in figure 2. Each curve represents numerical values of v'/Re for fixed $Re = 1, 2, \ldots, 32$. For a fixed δ it appears that the asymptotic behaviour when $Re \to \infty$ is determined by the presence or absence of channels. When channels are present ($\delta > 0$), then $v' \approx CRe$. When $\delta = 0$ (closed cellular flows) $v' \approx CRe^{\gamma}$, $\gamma > 1$. We study numerically and analytically the exponent γ of the power law in the next section.

3.2. *Closed cellular flows*

Here we establish asymptotic bounds for v' when $Re \to \infty$. The boundary value (cell) problem (3.3) whose solution determines this constant is similar to the cell problem that determines the effective diffusivity of a passive scalar for convection–diffusion by cellular flows. It was analysed in Fannjiang & Papanicolaou (1994) using a saddle-point variational principle. A generalization of this approach (see Appendix, § A.2) gives a variational principle for v' and provides rigorous bounds for it in the case of closed cellular flows. Combining (A 39) and (A 31), the asymptotic bounds for large Reynolds number for closed cellular flows are

$$0.02Re^{2.5} \leqslant v' \leqslant 0.109Re^{2.5}. \tag{3.6}$$

In figure 3 we show computed values of $\log v'$ for closed cellular flows ($\delta = 0$) with numerical error of order $0.001Re$. The numerical calculations indicate that for $55 \leqslant Re \leqslant 180$, v' can be sufficiently well approximated by

$$v' \approx 0.0668Re^{2.5}, \tag{3.7}$$

which is well within the theoretical bounds (3.6).

https://doi.org/10.1017/S0022112001005730 Published online by Cambridge University Press

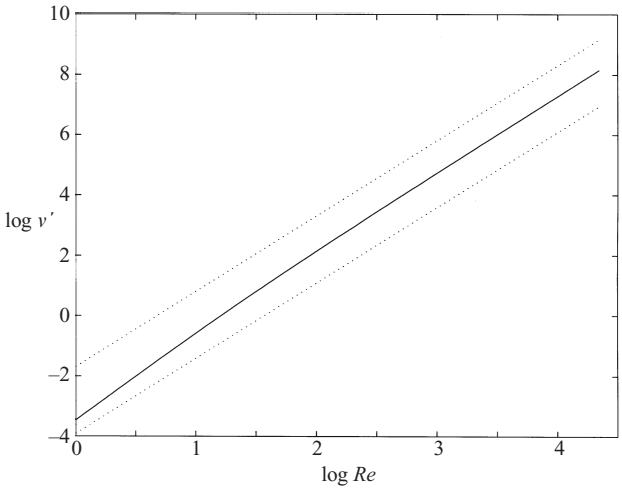


FIGURE 3. A plot of $\log v'$ as a function of $\log Re$ for $Re = 1, 2, \ldots, 77$. The dotted lines are the asymptotic bounds whose slope is 2.5.

4. Modulational stability analysis for cellular flows

4.1. *Linear stability*

Suppose that the nonlinear term in the modulation equation (3.1) is small compared to the linear terms. Then the behaviour of the solution is controlled by the tensor of eddy viscosity. Because of the different geometric structure of cellular flows with $\delta > 0$ and $\delta = 0$, linear stability of the large-scale perturbation is also different.

Consider a family of exponential solutions

$$\Psi(t, x) = \exp(\sigma t)\exp(k_1 x_1 + k_2 x_2). \tag{4.1}$$

The growth factor σ satisfies the dispersion relation

$$\sigma = \sigma(k_1, k_2) = -\frac{1}{Re}(k_1^2 + k_2^2)$$
$$+\frac{Re}{8}((k_1 + \delta k_2)^2 + (\delta k_1 + k_2)^2) - \left(\frac{Re}{2}(1 + \delta^2) + v'\right)\frac{(k_2^2 - k_1^2)^2}{k_1^2 + k_2^2}.$$

Clearly, for any δ there is modulational stability when

$$Re < \frac{2\sqrt{2}}{1 + \delta}.$$

As we have already remarked, the last term on the right-hand side of equation (3.1) always plays a stabilizing role. Using numerical values of v' (see figure 2) we can show that there is less instability of (4.1) for flows with smaller channels than for flows with bigger channels. The unstable solutions can be characterized in terms of the angle $\arctan(k_2/k_1)$. For any δ there is a set of angles $\arctan k_2/k_1$, for which the exponential solution (4.1) is unstable. This set is larger for flows with bigger channels; it is the smallest for closed cellular flows. Therefore, more isotropic flows are more stable. The shear flows ($\delta = 1$) are maximally unstable if the large-scale perturbation is perpendicular to the shear flow. This analysis was done for small Reynolds number in Sivashinsky & Yakhot (1985).

In the case of large Reynolds number, qualitatively the situation is similar. However,

https://doi.org/10.1017/S0022112001005730 Published online by Cambridge University Press

there is an important additional characteristic. Let us consider separately the two extreme cases: closed cellular flows ($\delta = 0$) and shear flows ($\delta = 1$).

For closed cellular flows the linearized equation for the large-scale stream function has the form

$$\frac{\partial \nabla^2 \Psi}{\partial t} = \left(\frac{1}{Re} - \frac{Re}{8}\right) \nabla^2 \nabla^2 \Psi + \left(\frac{Re}{2} + v'\right) (\nabla_2^2 - \nabla_1^2)^2 \Psi \tag{4.2}$$

with $v' \sim C_0 Re^{2.5}$ as $Re \to \infty$, by (3.6). We will use here the numerically computed value of C_0 from (3.7).

For shear flows, $v' = 0$ and the linearized equation for the large-scale stream function has the form

$$\frac{\partial \nabla^2 \Psi}{\partial t} = \frac{1}{Re} \nabla^2 \nabla^2 \Psi - \frac{Re}{4} (\nabla_1 + \nabla_2)^2 \nabla^2 \Psi + Re (\nabla_2^2 - \nabla_1^2)^2 \Psi. \tag{4.3}$$

For closed cellular flows the growth factor σ satisfies the dispersion relation

$$\sigma = \sigma(k_1, k_2) = \left(-\frac{1}{Re} + \frac{Re}{8}\right)(k_1^2 + k_2^2) - \left(\frac{Re}{2} + v'\right) \frac{(k_2^2 - k_1^2)^2}{k_1^2 + k_2^2}.$$

Instability, $\sigma(k_1, k_2) > 0$, occurs when

$$\left| \frac{1 - k_2^2/k_1^2}{1 + k_2^2/k_1^2} \right| < \frac{Re - 8/Re}{4Re + 8v'}. \tag{4.4}$$

Therefore, instability occurs when $k_2 = (1 \pm \beta(Re))k_1$ or $k_2 = (-1 \pm \beta(Re))k_1$, where β is sufficiently small. More precisely, if for large Re

$$|1 - k_2^2/k_1^2| < \beta^2(Re), \text{where asymptotically } \beta(Re) \approx 1.3679 Re^{-3/4}, \tag{4.5}$$

then exponential solutions with this (k_1, k_2) are unstable and they are stable otherwise. One can see that the set of unstable solutions for closed cellular flows depends significantly on the Reynolds number. In the limit $Re \to \infty$ negative eddy viscosity exists only for $k_1 = \pm k_2$, in other words the set of unstable solutions is almost empty.

For periodic shear flows and exponential solutions we have a different result. If for large Re

$$\tfrac{1}{3}(4 - \sqrt{7}) \leqslant \frac{k_2}{k_1} \leqslant \tfrac{1}{3}(4 + \sqrt{7}), \tag{4.6}$$

then exponential solutions are unstable and they are stable otherwise. Note that when the large-scale perturbation is parallel to the shear flow, the last two terms in equation (4.3) drop out and the solution behaves as if there were no eddies ($\phi = 0$).

We can analyse the behaviour of the eddy viscosity for small and large Reynolds numbers by considering the linear stability of modulational perturbations of cellular flows. For small Reynolds numbers (see Sivashinsky & Yakhot 1985), more isotropic small-scale closed cellular flows ($\delta = 0$) are more stable than shear cellular flows ($\delta = 1$) to large-scale perturbations. However, for small Reynolds numbers there are angular regions of wavenumbers where there are instabilities. When $Re = \infty$ the angular region of instabilities for closed cellular flows is almost empty (equation (4.5)). For shear cellular flows the angular region of instabilities is quite large (equation (4.6)).

4.2. *Nonlinear effects analysed numerically*

We now examine how the nonlinearity affects the linear stability results. We consider closed cellular flows but a similar analysis can be done for the whole family of

https://doi.org/10.1017/S0022112001005730 Published online by Cambridge University Press

cellular flows with the same results. We find numerically that the presence of the nonlinear terms does not affect stability. If the linearized equations are stable then the full equations are stable and if the linearized equations are unstable then the full equations develop instabilities as well.

For cellular flows equation (3.1) is

$$\frac{\partial \nabla^2 \Phi}{\partial t} + \frac{Re^2}{8}(\nabla_2^2 - \nabla_1^2)[\nabla_1 \Phi \nabla_2 \Phi] + J_{xx}(\Psi, \nabla^2 \Psi) = \left(\frac{1}{Re} - \frac{Re}{8}\right) \nabla^2 \nabla^2 \Phi + \left(\frac{Re}{2} + v'\right) (\nabla_2^2 - \nabla_1^2)^2 \Phi. \tag{4.7}$$

We solve this equation numerically on the square $S = [0,1] \times [0,1]$ with $1600 = 40 \times 40$ grid points and with homogeneous Dirichlet boundary conditions $\Phi_{\partial S} = 0$. We use an implicit Crank–Nicholson scheme for the stabilizing linear term and an explicit scheme for the nonlinear and destabilizing linear terms.

Linear instability arises when

$$\frac{1}{Re} - \frac{Re}{8} < 0.$$

Therefore the critical value of the Reynolds number for linear stability of the large-scale flows is $Re = 2\sqrt{2} \approx 2.8284$. When the Reynolds number is smaller than the critical value then the solutions are dissipative. When the Reynolds number is larger than the critical value then the dynamics is as follows. Quite rapidly the solution converges to a function which is almost in the kernel of the operator $(\nabla_2^2 - \nabla_1^2)^2$, and then instabilities start to develop.

Consider the linearly stable case. If the Reynolds number is small enough, then the Laplacian dominates all harmonic modes in the equation, even for very non-smooth initial data. In figure 4 the initial conditions were chosen to be a 40×40 matrix of random numbers independent and uniformly distributed on $[0,1]$, $Re = 1$ and we show how smooth the solution becomes after 100 time steps.

Consider the linearly unstable case. In figure 5 we show the evolution of the solution for $Re = 50$. We take the initial conditions to be a random linear combination of trigonometric functions. Even if the initial conditions are smooth, after 400 time steps, with $\Delta t = 0.01$, instabilities appear. Computations also show that, as expected from the linear stability analysis, the operator $(\frac{1}{2}Re + v')(\nabla_2^2 - \nabla_1^2)^2$ in (4.7) quite rapidly starts to dominate the other linear terms in all directions except for the ones close to the kernel of $(\nabla_2^2 - \nabla_1^2)^2$. So before the instabilities become visible the solution $\Psi(t,x)$ converges to the kernel of $(\nabla_2^2 - \nabla_1^2)^2$. In figure 5 (b) $(\nabla_2^2 - \nabla_1^2)\Phi$ is of order 10^{-3}.

The appearance of peaks in figure 5 (c) is due to the generation of large-wavenumber, unstable modes by the finite difference approximation of the differential operators. Note that small-wavenumber modes that are in the kernel of $(\nabla_2^2 - \nabla_1^2)^2$ also persist and grow.

5. Comparison with direct numerical simulations

We also carried out direct numerical simulation of perturbations of cellular flows on a square with periodic boundary conditions, that is we solved numerically the linearized equation

$$\partial_t \nabla^2 \tilde{\Phi}^\epsilon(t,x) = \frac{1}{Re} \nabla^2 \nabla^2 \tilde{\Phi}^\epsilon(t,x) - J_{xx}\left(\phi\left(\frac{x}{\epsilon}\right), \left(\frac{2}{\epsilon^2} + \nabla^2\right) \tilde{\Phi}^\epsilon(t,x)\right), \; t \in [0,1]. \tag{5.1}$$

https://doi.org/10.1017/S0022112001005730 Published online by Cambridge University Press

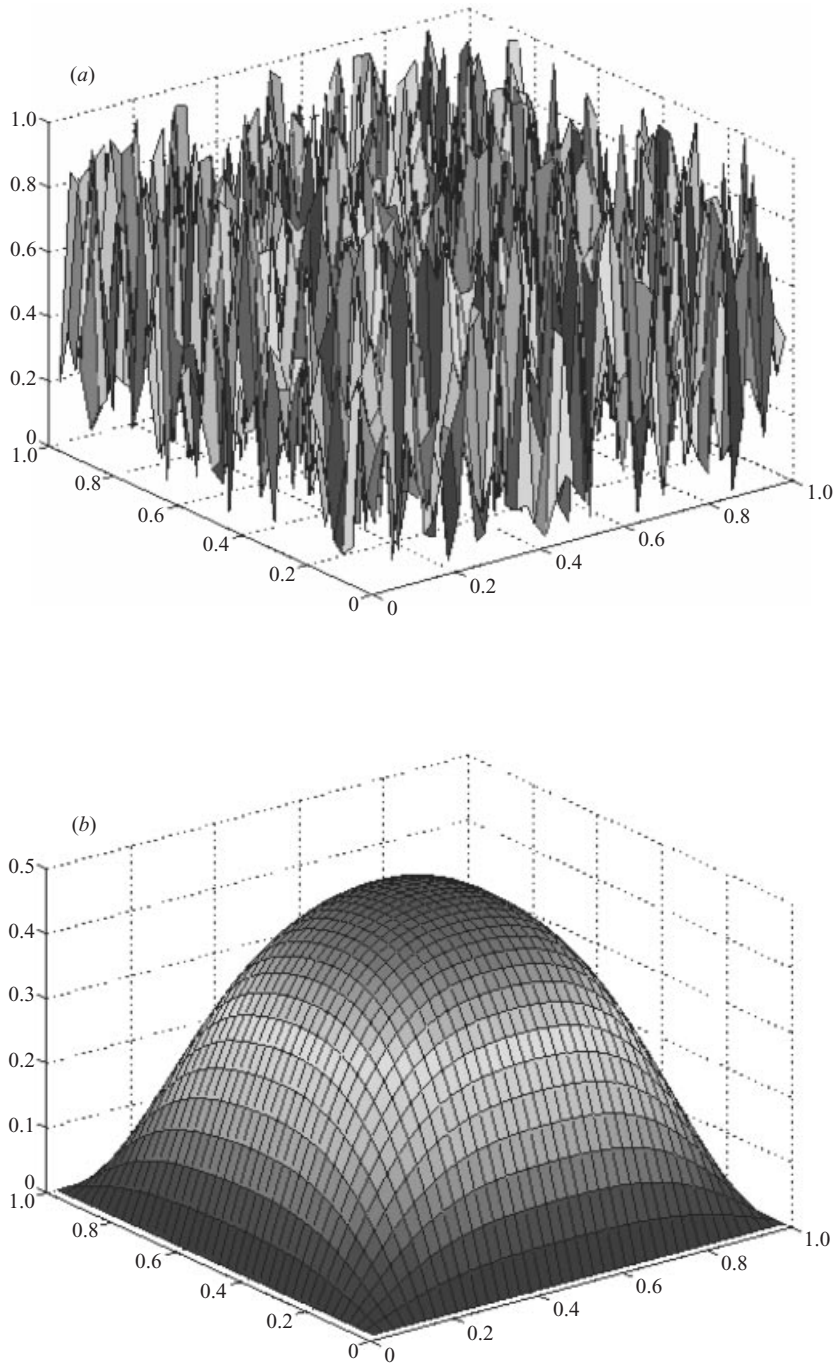


FIGURE 4. Linearly stable case ($Re = 1$) with the initial condition shown in (a) and the solution after 100 time-steps ($\Delta t = 0.1$) shown in (b).

We compared for very small ϵ (between 0.1 and 0.0001) the solutions with the predictions of the multiscale analysis. For these ϵ the largest Reynolds number for which the solutions are bounded uniformly in ϵ is seen numerically to be essentially independent of ϵ. For different initial conditions the solutions at time $t = 1$ exhibit the

https://doi.org/10.1017/S0022112001005730 Published online by Cambridge University Press

phenomena of depleted, enhanced or negative viscosity that confirm the non-isotropic tensor nature of eddy viscosity with good qualitative and quantitative agreement with the multiscale analysis.

The details of the numerical method will be reported elsewhere by the first author. Here we summarize the results. We approximate the solution by taking finitely many Fourier coefficients. We show that the number of Fourier coefficients can be taken for a fixed Re independent of ϵ because, by the discrete maximum principle for the absolute values of Fourier coefficients, we can control the L_2-norm of the truncation error uniformly in ϵ. We observe that the algorithm converges for any Reynolds numbers only for closed cellular flows ($\delta = 0$). Therefore the closed cellular flows are the most stable in the family of cellular flows.

We show that with initial conditions of the form

$$\tilde{\Phi}^{\epsilon}(t,x)|_{t=0} = \cos(mx_1 + nx_2), \tag{5.2}$$

for $t \in [0,1]$, all Fourier coefficients corresponding to the 'small-scale' modes of solution of (5.1) are negligible, with an L_2-norm less than 10^{-7}. Therefore

$$\tilde{\Phi}^{\epsilon}(t,x) \approx C(t)\cos(mx_1 + nx_2). \tag{5.3}$$

In figure 6 we show the results of numerical experiments that confirm the anisotropic tensorial structure of eddy viscosity. The numerical results agree qualitatively and quantitatively with the expected behaviour of the large-scale perturbations. The initial conditions are given by (5.2), where the pair (m,n) takes 5 different values:

$$\left.\begin{array}{lrr} \text{(i)} & m = 1/\sqrt{2}, & n = 1/\sqrt{2}, \\ \text{(ii)} & m = -1/\sqrt{2}, & n = 1/\sqrt{2}, \\ \text{(iii)} & m = 0, & n = 1, \\ \text{(iv)} & m = 0.5, & n = \sqrt{0.75}, \\ \text{(v)} & m = -0.5, & n = \sqrt{0.75}. \end{array}\right\} \tag{5.4}$$

We plot the 'large-scale' coefficient $C(t)$ of (5.3) at $t = 1$ as a function of δ between 0 and 1. We take $m^2 + n^2 = 1$. This conveniently allows us to put the results of the numerical simulations in one figure. The numbering in figure 6 corresponds to that of the initial conditions (5.4). The dashed line corresponds to the value of the large-scale Fourier coefficient with no convection term. Therefore if a curve, or a part of a curve is below the dashed line, then the viscosity is enhanced by the presence of convection; if a curve, or a part of a curve is above the dashed line, then the viscosity is depleted by the presence of convection.

Our numerical results confirm the linear analysis in § 4.1. Curve (iii) corresponds to the case when the solution is only a function of x_2. The linear analysis predicts that this is the case of the maximally enhanced viscosity for any δ. Curve (i) corresponds to the case when the solution is perpendicular to the channels. The linear analysis predicts that this is the case of maximally depleted viscosity. Curve (ii) corresponds to the case when the solution is parallel to the channels. The linear analysis predicts that this is the case of the maximally depleted viscosity in the absence of channels ($\delta = 0$); for the shear flows ($\delta = 1$) it predicts that the eddy viscous corrections should not be observable. The initial conditions for curves (iv) and (v) are intermediate. We observe depleted viscosity for small channels and enhanced viscosity for large channels for $m = -0.5, n = \sqrt{0.75}$ (curve v).

https://doi.org/10.1017/S0022112001005730 Published online by Cambridge University Press

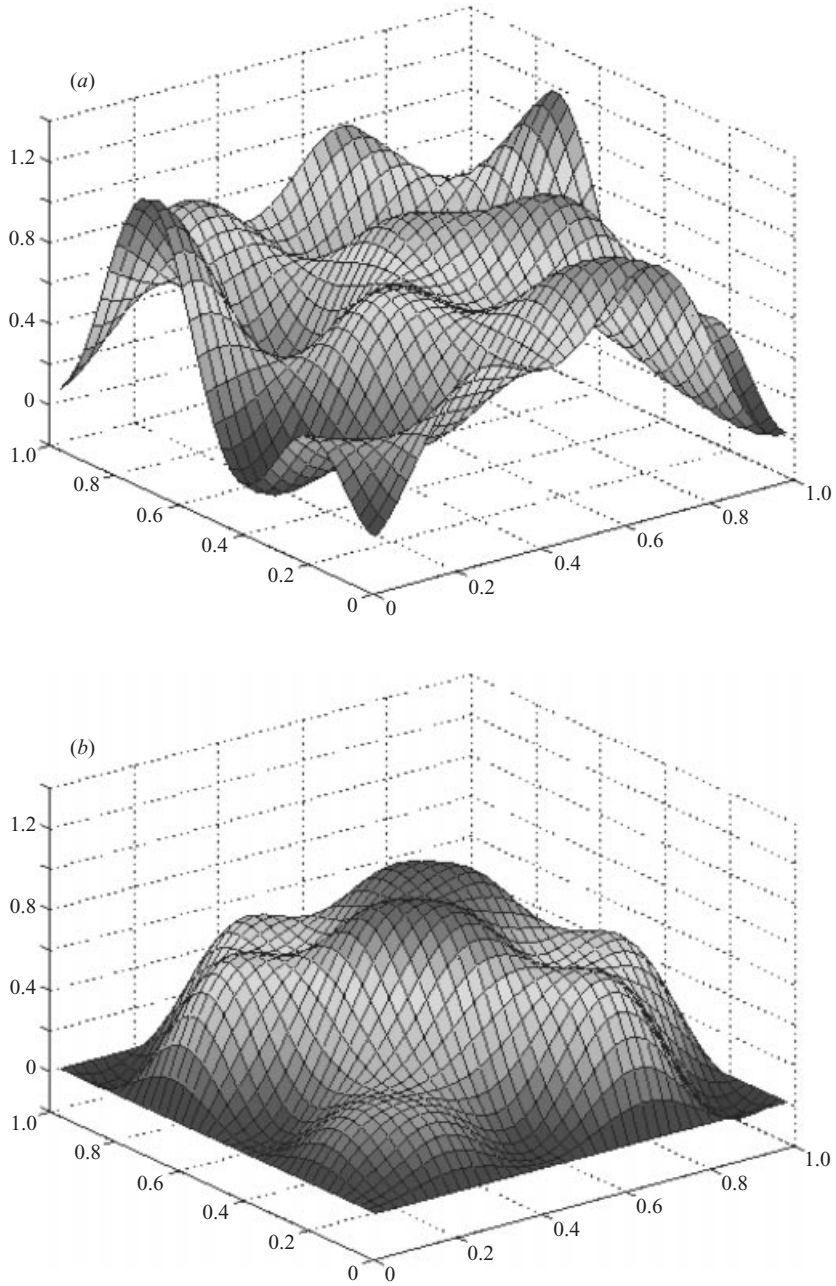


FIGURE 5(*a*, *b*). For caption see facing page.

6. Concluding remarks

We have analysed the behaviour of large-scale perturbations of small-scale eddies and have shown that the geometrical structure of the eddies plays an important role in the effective equations of large-scale transport. The behaviour of large-scale perturbations at high Reynolds numbers is more stable when the underlying eddies have closed streamlines. The model we consider here is the simplest one that shows

https://doi.org/10.1017/S0022112001005730 Published online by Cambridge University Press

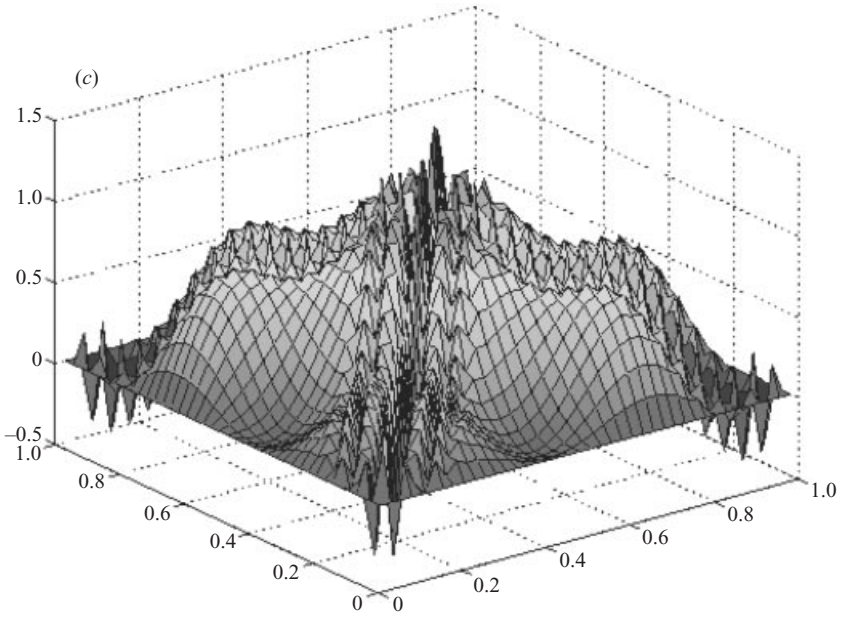


FIGURE 5. Nonlinear solutions with $Re = 50$: (a) the initial stream function, (b) after 200 time steps and (c) after 400 time steps, with $\Delta t = 0.1$.

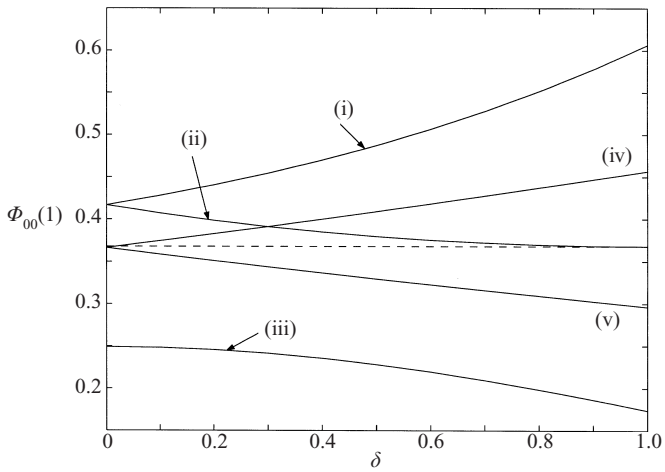


FIGURE 6. The large-scale Fourier coefficient $C(t)$ at $t = 1$, $\epsilon = 0.01$ as a function of δ. The dashed line is this coefficient without the convective term ($\phi = 0$).

this behaviour. The theory can be generalized in several directions. The derivation of the tensor of eddy viscosities by multiscale analysis can be carried out in the β-plane approximation for geostrophic flows. As already remarked, among cellular flows those with no channels (closed cellular flows) play a distinct role – they are the most linearly stable. This may explain the persistence of these cell-like mesoscale ocean flows (see Cushman-Roisin *et al.* 1984).

The strict separation of scales needed for homogenization is physically unrealistic. However, when flows with a large number of scales are involved one can think

https://doi.org/10.1017/S0022112001005730 Published online by Cambridge University Press

of using homogenization iteratively from one scale to the next less fine one to get overall large-scale dynamics. This more realistic analysis remains to be done for flows. Iterated homogenization has been carried out in other, linear contexts (see Bensoussan, Lions & Papanicolaou 1978).

Another direction is to consider more general small-scale eddies. We believe that a similar technique, that is deformation of linear elliptic operators and variational principles, can be used to extend the results to the random cellular flows analysed in Fannjiang & Papanicolaou (1997) and Isichenko (1992) for the convection–diffusion of passive scalars.

Work supported by grants AFOSR F49620-98-1-0211 and NSF-DMS-9971972.

Appendix. Variational bounds for closed cellular flows

A.1. *Introduction*

The cell problem (3.3) is a fourth order operator with variable coefficients. There is no closed analytical solution for this equation. However, we are not interested in the explicit solution but only in v' defined by (3.2) when $Re \to \infty$. In order to estimate v' we will introduce saddle-point variational principles for it.

Let us first put equation (3.3) in divergence form because it will be important for the variational formulation. Note that the term $J_{yy}(\phi, (\Delta + 2)\psi + Re\, e)$ with

$$e = -\frac{\partial_1 \partial_2 \phi}{2}. \tag{A 1}$$

is antisymmetric as a function of

$$\chi = \Delta\psi + 2\psi\ . \tag{A 2}$$

We can write

$$\Delta\Delta\psi = \Delta S\chi$$

with S a symmetric nonlocal linear operator defined by

$$S\psi = (\Delta + 2)^{-1}\Delta\psi. \tag{A 3}$$

The operator S is not well-defined if $\Delta\psi = -2\psi$ and it is not positive definite where it is well-defined. However if χ and ψ lie in a subspace of periodic mean-zero H^1 functions $\mathscr{L} \subset H^1(\square)$, defined by

$$\mathscr{L} = \{\psi | (\Delta + 2)\psi = 0, (\Delta + 1)\psi = 0\}^{\perp}, \tag{A 4}$$

then S is a well-defined positive-definite continuous operator. The solution ψ of the cell problem (3.3) can be split into two parts

$$\psi = \psi' + \psi'', \qquad \psi' \in \mathscr{L}, \qquad \psi'' \in \mathscr{L}^{\perp}. \tag{A 5}$$

Since the solution of equation (3.3) satisfies (3.4) we have

$$\psi'' = C\partial_1 \partial_2 \phi \tag{A 6}$$

with some unknown constant C. Define $\boldsymbol{S}$ and $\boldsymbol{H}$ by

$$\frac{1}{Re}\boldsymbol{S} + \boldsymbol{H} = \frac{1}{Re}\begin{pmatrix} S & 0 \\ 0 & S \end{pmatrix} + \begin{pmatrix} 0 & -\phi \\ \phi & 0 \end{pmatrix} = \begin{pmatrix} S/Re & -\phi \\ \phi & S/Re \end{pmatrix}. \tag{A 7}$$

https://doi.org/10.1017/S0022112001005730 Published online by Cambridge University Press

Then the cell problem (3.3) is equivalent to

$$\partial \cdot \left(\frac{1}{Re} \boldsymbol{S} + \boldsymbol{H} \right) \partial(\chi + Re\, e) = \lambda \partial_1 \partial_2 \phi, \quad \chi \in \mathscr{L}, \tag{A 8}$$

where

$$\lambda = -\langle \psi \partial_1 \partial_2 \phi \rangle \frac{1}{Re}. \tag{A 9}$$

The cell problem (A 8) is similar in form to the one for the convection–diffusion problem of cellular flows considered by Fannjiang & Papanicolaou (1994) (see also the complex conductivity problem discussed in Cherkaev & Gibiansky 1994). The cell problem for convection–diffusion of cellular flows is

$$\partial \cdot \begin{pmatrix} 1/Pe & -\phi(y) \\ \phi(y) & 1/Pe \end{pmatrix} \partial(\chi + e) = 0, \tag{A 10}$$

where χ is a mean-zero periodic function of two variables, $e = y_1$, and Pe is the Péclet number, which is assumed to be large. We use their symmetrization technique in deriving a saddle-point energy functional and variational principles. The coefficient λ in (A 8) arises naturally as a Lagrange multiplier for the constraint $\chi \in \mathscr{L}$. Two important conditions that allowed Fannjiang & Papanicolaou (1994) to derive the saddle-point variational principle by symmetrization are: that the differential operator is in divergence form and that its symmetric part is positive-definite. Note that by introducing the non-local operator $\boldsymbol{S}$ we wrote equation (3.3) in divergence form, where the symmetric part of the operator is positive-definite. The price we pay for this representation is that the solution must belong to the subspace $\mathscr{L} \subset H^1(\square)$ (see equation (A 4)), and that the right-hand side of equation (A 8) is some function from $\mathscr{L}^{\perp}$.

A.2. *Variational principle by symmetrization*

For equation (A 8) introduce the adjoint problem

$$\partial \cdot \left(\frac{1}{Re} \boldsymbol{S} - \boldsymbol{H} \right) (\partial(\chi' + Re\, e) = \lambda' \partial_1 \partial_2 \phi, \quad \chi' \in \mathscr{L}. \tag{A 11}$$

The λ' will be identified later as a Lagrange multiplier for $\partial_1 \partial_2 \phi$. It is not known *a priori* that in equation (A 11) there are no other Lagrange multipliers, but this follows from the symmetries (3.4) of the adjoint problem. With the change of variables (symmetrization)

$$\chi^{\pm} = \frac{\chi \pm \chi'}{2}, \tag{A 12}$$

equations (A 8) and (A 11) are transformed into coupled equations for the functions $\chi^{\pm}$

$$\frac{1}{Re} \partial \cdot \boldsymbol{S} \partial \chi^{+} + \partial \cdot \boldsymbol{H} \partial \chi^{-} = \lambda^{+} \partial_1 \partial_2 \phi, \quad \chi^{+}, \chi^{-} \in \mathscr{L}, \tag{A 13}$$

$$\frac{1}{Re} \partial \cdot \boldsymbol{S} \partial \chi^{-} + \partial \cdot \boldsymbol{H} \partial(\chi^{+} + Re\, e) = \lambda^{-} \partial_1 \partial_2 \phi, \quad \chi^{+}, \chi^{-} \in \mathscr{L}. \tag{A 14}$$

For any pair of periodic mean-zero functions $\hat{\chi}^{+} \in \mathscr{L}$ and $\hat{\chi}^{-} \in \mathscr{L}$, following Fannjiang & Papanicolaou (1994), consider the *energy functional*

$$U(\hat{\chi}^{+}, \hat{\chi}^{-}, e) = \frac{1}{Re} \langle \partial \hat{\chi}^{+} \cdot \boldsymbol{S} \partial \hat{\chi}^{+} \rangle - \frac{1}{Re} \langle \partial \hat{\chi}^{-} \cdot \boldsymbol{S} \partial \hat{\chi}^{-} \rangle + 2 \langle \partial(\hat{\chi}^{+} + Re\, e) \boldsymbol{H} \partial \hat{\chi}^{-} \rangle. \tag{A 15}$$

https://doi.org/10.1017/S0022112001005730 Published online by Cambridge University Press

In the problem of convection–diffusion, the extremal value of a similarly defined energy functional is the effective diffusivity. It was shown in Fannjiang & Papanicolaou (1994) how to obtain rigorous bounds using saddle-point variational principles. In our case by direct computation the extremal value of the energy functional is

$$U(\chi^+, \chi^-, e) = \frac{v'}{2}. \tag{A 16}$$

This allows us to use variational techniques to obtain bounds for v'. We have the following saddle-point variational principle

THEOREM A.1. *The value at the unique saddle-point of the quadratic energy functional* $U(\hat{\chi}^+, \hat{\chi}^-, e)$ *is*

$$\frac{v'}{2} = \inf_{\hat{\chi}^+ \in \mathscr{L}} \sup_{\hat{\chi}^- \in \mathscr{L}} U(\hat{\chi}^+, \hat{\chi}^-, e). \tag{A 17}$$

The classical methods of the calculus of variations (see for example Gelfand & Fomin 1963) give the Euler–Lagrange equations

$$\left.\begin{aligned} \frac{1}{Re}\partial \cdot \boldsymbol{S}\partial\chi^+ + \partial \cdot \boldsymbol{H}\partial\chi^- &= \sum_i \lambda_i^+ \mu_i, \quad \chi^+, \chi^- \in \mathscr{L}, \\ \frac{1}{Re}\partial \cdot \boldsymbol{S}\partial\chi^- + \partial \cdot \boldsymbol{H}\partial\chi^+ &= \sum_i \lambda_i^- \mu_i, \quad \chi^+, \chi^- \in \mathscr{L}. \end{aligned}\right\} \tag{A 18}$$

The functions $\mu_i(y)$ span the linear space $\mathscr{L}^\perp$:

$$\mathscr{L}^\perp = \operatorname{span}\{\mu_i(y)\}. \tag{A 19}$$

Equations (A 18) are exactly (A 13) and (A 14) because of the symmetries (3.4). Equation (A 17) follows immediately from (A 16).

The use of symmetrization here and in similar problems leads to a non-degenerate variational principle. Symmetrization is analogous to rotation by $\frac{1}{4}\pi$ in the plane applied to hyperboloids $z = xy$ to give the form $z = x^2 - y^2$. In fact, (A 15) in the old variables $\hat{\chi}$ and $\hat{\chi}'$ has the form

$$U(\hat{\chi}, \hat{\chi}', e) = \langle \partial(\hat{\chi}' + e) \cdot (\boldsymbol{S} + \boldsymbol{H})\partial(\hat{\chi} + e) \rangle \tag{A 20}$$

and the second variation with respect to variables $\hat{\chi}$ and $\hat{\chi}'$ is identically zero. By analogy to rotation in the plane we have chosen the particular change of variables (A 12) and obtained a non-degenerate energy functional. There are many other changes of variables that can be used and their choice is dictated by the applications of the variational principle. For example, Milton (1990) analysed the group of changes of variables for elasticity, which is analogous to rotation by an arbitrary angle.

A.3. *Bounds from the variational principle*

It appears at first that the saddle-point variational formulation for v' is more complicated than the original cell problem (3.3). Nevertheless, by means of the variational principle we can construct tight estimates for v' for closed cellular flows $\phi = \sin y_1 \sin y_2$ and large Re. The bounds are optimal in the Reynolds number but the numerical constants for the upper and lower bound are not optimal and can be improved by more careful estimates.

The method is as follows. The value of the energy integral (A 15) at the saddle-point equals $\frac{1}{2}v'$ by theorem A.1. For an arbitrary fixed trial function $\chi^-_{lower} \in \mathscr{L}$, the

https://doi.org/10.1017/S0022112001005730 Published online by Cambridge University Press

minimum over all $\hat{\chi}^+ \in \mathscr{L}$ of the energy integral $U(\hat{\chi}^+, \chi^-_{lower}, e)$ is certainly less than $\frac{1}{2}v'$. If $\phi = \sin y_1 \sin y_2$ then there is an additional property of solutions of (A 18)

$$\chi^{\pm} = \sum_{k\,l} a_{k\,l} \cos ky_1 \cos ly_2. \tag{A 21}$$

Choose χ^-_{lower} to be a truncated series of the form (A 21):

$$\chi^-_{lower} = \boldsymbol{C}\chi = \boldsymbol{C} \sum_{k\,l \leqslant N} a_{k\,l} \cos ky_1 \cos ly_2, \tag{A 22}$$

where $\boldsymbol{C}$, N and $a_{k\,l}$ depend on Re. The minimum of $U(\hat{\chi}^+, \chi^-_{lower}, e)$ is achieved when $\hat{\chi}^+ = \chi^+_{lower}$ satisfies the Euler–Lagrange equation

$$\frac{1}{Re}\partial \cdot \boldsymbol{S}\partial\chi^+_{lower} = -\partial \cdot \boldsymbol{H}\partial\chi^-_{lower} + \sum_i \lambda_i\mu_i \tag{A 23}$$

where λ_i are Lagrange multipliers for the constraint $\chi^+_{lower} \in \mathscr{L}$ and μ_i are defined in (A 19). Given χ^-_{lower}, this equation is easy to solve. If the right-hand side of (A 23) is expanded in Fourier series

$$-\partial \cdot \boldsymbol{H}\partial\chi^-_{lower} = \boldsymbol{C} \sum_{0 \leqslant k\,l \leqslant N} b_{k\,l} \cos ky_1 \cos ly_2 \,(k\,l \text{ integers}),$$

equations (A 23) are explicitly solved by

$$\chi^+_{lower} = \boldsymbol{C}Re \sum_{0 \leqslant k\,l \leqslant N} b_{k\,l} \left(1 - \frac{2}{k^2 + l^2}\right) (k^2 + l^2)^{-1} \cos ky_1 \cos ly_2.$$

We have

$$\frac{1}{Re}\langle \partial\chi^+_{lower} \cdot \boldsymbol{S}\partial\chi^+_{lower}\rangle = \langle \partial\chi^+_{lower} \cdot \boldsymbol{H}\partial\chi^-_{lower}\rangle \sim Re\ \boldsymbol{C}^2 \langle \boldsymbol{H}\partial\chi \cdot \boldsymbol{S}^{-1}\boldsymbol{H}\partial\chi\rangle. \tag{A 24}$$

We will choose χ so that $\partial \cdot \boldsymbol{H}\partial\chi \notin \mathscr{L}$ and then

$$\boldsymbol{S}^{-1}\boldsymbol{H}\partial\chi \neq \partial\chi',$$

χ' satisfies

$$\Delta S\chi' = -\partial \cdot \boldsymbol{H}\partial\chi + \sum_i \lambda_i\mu_i.$$

Thus, choosing a trial function $\chi^-_{lower} \in \mathscr{L}$ as in (A 22) and solving (A 23) for χ^+_{lower} exactly we have

$$2\boldsymbol{C}Re\langle \partial e \cdot \boldsymbol{H}\partial\chi\rangle - \boldsymbol{C}^2 \left(Re\langle \boldsymbol{H}\partial\chi \cdot \boldsymbol{S}^{-1}\boldsymbol{H}\partial\chi\rangle + \frac{1}{Re}\langle \partial\chi \cdot \boldsymbol{S}\partial\chi\rangle \right) \leqslant \frac{v'}{2}. \tag{A 25}$$

The choice of N in (A 22) is optimal if

$$Re\langle \boldsymbol{H}\partial\chi \cdot \boldsymbol{S}^{-1}\boldsymbol{H}\partial\chi\rangle \sim \frac{1}{Re}\langle \partial\chi \cdot \boldsymbol{S}\partial\chi\rangle. \tag{A 26}$$

The choice of $\boldsymbol{C}$ is optimal if

$$2\boldsymbol{C}Re\langle \partial e \cdot \boldsymbol{H}\partial\chi\rangle \sim \boldsymbol{C}^2 \left(Re\langle \boldsymbol{H}\partial\chi \cdot \boldsymbol{S}^{-1}\boldsymbol{H}\partial\chi\rangle + \frac{1}{Re}\langle \partial\chi \cdot \boldsymbol{S}\partial\chi\rangle \right). \tag{A 27}$$

The choice of χ is the most difficult part of the construction. We cannot give a simple

https://doi.org/10.1017/S0022112001005730 Published online by Cambridge University Press

algorithm for choosing it. It is motivated by the observation that (A 26) holds if χ is almost in the kernel of operator $\partial \cdot \boldsymbol{H} \partial(\chi)$.

For the upper bound the procedure is reversed. We choose $\chi^+_{upper} \in \mathscr{L}$ so that

$$\chi^+_{lower} + Re\, e = Re \sum_{k\,l \leqslant N} a_{k\,l} \cos ky_1 \cos ly_2, \tag{A 28}$$

solve exactly for χ^-_{upper} the Euler–Lagrange equations, similar to (A 23), and as in (A 25) we have

$$\frac{v'}{2} \leqslant \frac{1}{Re} \langle \partial \chi^+_{lower} \boldsymbol{S} \partial \chi^+_{lower} \rangle + Re \langle \boldsymbol{H} \partial (\chi^+_{lower} + Re\, e \cdot \boldsymbol{S}^{-1} \boldsymbol{H} \partial (\chi^+_{lower} + Re\, e) \rangle. \tag{A 29}$$

Note that for the upper bound in (A 28) we do not have a constant $\boldsymbol{C}$ as in (A 22). Another difference is that $\boldsymbol{S}^{-1} \boldsymbol{H} \partial (\chi^+ + Re\, e)$ will be well-defined, because we will choose χ^+ such that $\partial \cdot \boldsymbol{H} \partial (\chi^+ + Re\, e) \in \mathscr{L}$.

A.4. *Lower bound*

For the upper and lower bounds we use the relations

$$\langle \cos^2(my_1) \cos^2(ny_2) \rangle = 1/4, \quad \langle \cos^2(my_1) \rangle = 1/2, \tag{A 30a, b}$$

$$\|S\| = 2, \quad ||S^{-1}|| = 1. \tag{A 30c, d}$$

THEOREM A.2. *For closed cellular flows, when Re is large we have the lower bound*

$$\frac{15^{3/4}}{256\sqrt{2}} Re^{2.5} \approx 0.02 Re^{2.5} \leqslant v'. \tag{A 31}$$

Proof. Suppose a trial function χ^-_{lower} is

$$\chi^-_{lower} = \boldsymbol{C} \sum_{k=1}^{N} \left(1 - \frac{k^2}{N^2}\right) \frac{\cos(2ky_1)}{2k}, \tag{A 32}$$

where the constant $\boldsymbol{C}$ is chosen appropriately later. By inspection it is admissible, that is $\chi^-_{lower} \in \mathscr{L}$, and

$$2 \langle \partial e \cdot \boldsymbol{H} \partial \chi^-_{lower} \rangle = \frac{Re^2 \boldsymbol{C}}{4} \left(1 - \frac{1}{N^2}\right) \langle \cos^2(2y_1) \rangle \sim \frac{Re \boldsymbol{C}}{8} \tag{A 33}$$

by (A 30*b*). The Euler–Lagrange equation (A 23) for χ^+_{lower} is

$$\begin{aligned} \frac{1}{Re} \partial \cdot \boldsymbol{S} \partial \chi^+_{lower} &= \boldsymbol{C} \sin y_1 \cos y_2 \sum_{k=1}^{N} \left(1 - \frac{k^2}{N^2}\right) \sin(2ky_1) + \sum_i \lambda_i \mu_i \\ &= \frac{\boldsymbol{C}}{2} \left(1 - \frac{1}{N^2}\right) \cos y_1 \cos y_2 - \frac{\boldsymbol{C} \cos y_2}{2} \sum_{k=1}^{N} \frac{2k-1}{N^2} \cos((2k-1)y_1) \\ &\quad + \sum_i \lambda_i \mu_i \\ &= -\frac{\boldsymbol{C} \cos y_2}{2} \sum_{k=0}^{N-1} \frac{2k+1}{N^2} \cos((2k+1)y_1), \end{aligned} \tag{A 34}$$

https://doi.org/10.1017/S0022112001005730 Published online by Cambridge University Press

where λ_i are Lagrange multipliers of the constraints (A 4). Note that the term

$$\frac{\boldsymbol{C}}{2}\left(1-\frac{1}{N^2}\right)\cos y_1 \cos y_2 \in \mathscr{L}^{\perp}$$

and it is absorbed into $\sum_i \lambda_i \mu_i$. So

$$\chi^{+}_{lower} = -\frac{Re\boldsymbol{C}}{2N^2}\sum_{k=1}^{N-1}\left[1-\frac{2}{(2k+1)^2+1}\right]\frac{2k+1}{(2k+1)^2+1}\cos((2k+1)y_1)\cos y_2. \quad \text{(A 35)}$$

Therefore by (A 30 a, d)

$$\begin{aligned}\frac{1}{Re}\langle \partial\chi^{+}_{lower}\cdot \boldsymbol{S}\partial\chi^{+}_{lower}\rangle &= \langle \partial\chi^{+}_{lower}\cdot \boldsymbol{H}\partial\chi^{-}_{lower}\rangle \\ &\leqslant \frac{Re\boldsymbol{C}^2}{16N^4}\sum_{k=1}^{N-1}\frac{(2k+1)^2}{(2k+1)^2+1} \leqslant \frac{Re\boldsymbol{C}^2}{16N^3} \end{aligned} \quad \text{(A 36)}$$

we also have with (A 30 a, c)

$$\begin{aligned}\frac{1}{Re}\langle \partial\chi^{-}_{lower}\cdot \boldsymbol{S}\partial\chi^{-}_{lower}\rangle &\leqslant 2\frac{\boldsymbol{C}^2}{Re}\sum_{k=1}^{N}\left[1-\frac{k^2}{N^2}\right]^2\langle \sin^2(2ky_1)\rangle \\ &\leqslant \frac{\boldsymbol{C}^2}{Re}\sum_{k=1}^{N}\left[1-\frac{k^2}{N^2}\right]^2 \leqslant \frac{8N\boldsymbol{C}^2}{15Re}. \end{aligned} \quad \text{(A 37)}$$

Combining (A 36), (A 37) and (A 33), we have

$$U(\chi^{+}_{lower}, \chi^{-}_{lower}, e) \geqslant \frac{Re\boldsymbol{C}}{8} - \frac{Re\boldsymbol{C}^2}{16N^3} - \frac{8N\boldsymbol{C}^2}{15Re}.$$

For the optimal choice of N and $\boldsymbol{C}$

$$N = \sqrt{Re}\left(\frac{15}{128}\right)^{1/4}, \quad \boldsymbol{C} = Re^{1.5}\frac{30^{3/4}}{128}$$

we have

$$\frac{v'}{2} \geqslant \frac{30^{3/4}}{2048}Re^{2.5} \approx 0.01Re^{2.5}. \quad \text{(A 38)}$$

□

A.5. *Upper bound*

THEOREM A.3. *For closed cellular flows, when $Re \to \infty$ we have the upper bound*

$$v' \leqslant 2 * 48^{-3/4}Re^{2.5} \approx 0.109Re^{2.5}. \quad \text{(A 39)}$$

Proof. Take the trial function χ^{+}_{upper}, such that

$$\chi^{+}_{upper} + Re\, e = \frac{Re}{2}\sum_{m,n\geqslant 0, m*n<N}\left(1-\frac{mn}{N}\right)^2\cos(2m+1)y_1\cos(2n+1)y_2.$$

For this trial function we can obtain sufficiently good estimates for χ^{-}. This follows from

https://doi.org/10.1017/S0022112001005730 Published online by Cambridge University Press

LEMMA 1. *If $m, n \neq 0$, then*

$$\langle \cos(2my_1)\cos(2ny_2) J_{yy}(\phi, \chi^+ + Re\, e)\rangle = \frac{Re}{4}\frac{m^2 - n^2}{N^2}.$$

If $n = 0$ then

$$\langle \cos(2my_1) J_{yy}(\phi, \chi^+ + Re\, e)\rangle = \frac{Re}{4}\frac{m^2 - m}{N^2}.$$

If $m * n \approx N$, and $m \geqslant n$ then

$$|\langle \cos(2my_1)\cos(2ny_2) J_{yy}(\phi, \chi^+ + Re\, e)\rangle| \leqslant Re\frac{1}{n}.$$

The equalities follow from direct computations and (A 30*a*, *b*). The inequality also follows from direct computations, but one has to analyse three cases: the number of non-zero coefficients that contribute to the Fourier coefficient of $\cos(2my_1)\cos(2ny_2)$ can be one, two or three.

The function χ^-_{upper} can be given explicitly in terms of Fourier series by solving the Euler–Lagrange equations and by (A 30*a*, *b*, *d*):

$$\frac{1}{Re}\langle \partial\chi^-_{upper} \cdot \boldsymbol{S} \partial\chi^-_{upper}\rangle \leqslant \frac{Re^3}{16N^4} \sum_{0\leqslant m,n\leqslant N, m*n<N} \frac{(m^2-n^2)^2}{m^2+n^2} + \frac{Re^3}{8} \sum_{m*n\approx N, m\geqslant n} \frac{1}{(m^2+n^2)n^2}. \tag{A 40}$$

Consider the first term in (A 40). Using

$$\frac{(m^2-n^2)^2}{m^2+n^2} \leqslant \frac{(x^2-y^2)^2}{x^2+y^2} + 8(x+y+1), \quad 1 \leqslant m \leqslant x < m+1, \quad 1 \leqslant n \leqslant y < n+1,$$

we have an integral bound

$$\frac{Re^3}{16N^4} \sum_{0\leqslant m,n\leqslant N, m*n<N} \frac{(m^2-n^2)^2}{m^2+n^2} \leqslant \frac{Re^3}{16N^4} \left[\iint_{\substack{1<x,y<N+1 \\ x*y<N+1}} \frac{(x^2-y^2)^2}{x^2+y^2} \mathrm{d}x\mathrm{d}y + \iint_{\substack{1<x,y<N+1 \\ x*y<N+1}} 8(x+y+1)\,\mathrm{d}x\mathrm{d}y \right]. \tag{A 41}$$

The second term in (A 41) is asymptotically small compared to the first term

$$\frac{Re^3}{16N^4} \iint_{\substack{1<x,y<N+1 \\ x*y<N+1}} 8(x+y+1)\,\mathrm{d}x\mathrm{d}y \leqslant \frac{2Re^3}{N^4} \iint_{\substack{1<y<(N+1)/x \\ 1<x<N+1}} x\mathrm{d}y\mathrm{d}x \leqslant \frac{Re^3}{N^2}.$$

For the first term in (A 41) we use the change of variables

$$\tilde{y} = x^2 - y^2, \quad \tilde{x} = x * y$$

https://doi.org/10.1017/S0022112001005730 Published online by Cambridge University Press

with the Jacobian

$$|J| = \left| \frac{\partial \tilde{x}}{\partial x}\frac{\partial \tilde{y}}{\partial y} - \frac{\partial \tilde{y}}{\partial x}\frac{\partial \tilde{x}}{\partial y} \right| = 0.5\frac{1}{x^2+y^2}$$

and have an estimate

$$\frac{Re^3}{16N^4}\iint \frac{(x^2-y^2)^2}{x^2+y^2}\mathrm{d}x\mathrm{d}y \leqslant \frac{Re^3}{32N^4}\iint_{\substack{-\tilde{x}^2<\tilde{y}<\tilde{x}^2 \\ 1<\tilde{x}<N+1}} \frac{(x^2-y^2)^2}{(x^2+y^2)^2}\mathrm{d}\tilde{x}\mathrm{d}\tilde{y}$$

$$\leqslant \frac{Re^3}{32N^4}\int_{1<\tilde{x}<N} \tilde{x}^2 d\tilde{x} \leqslant \frac{Re^3}{96N}.$$

Consider the second term in (A 40). Using $mn \approx N$ we have

$$\frac{Re^3}{8}\sum_{m*n\approx N, m\geqslant n}\frac{1}{(m^2+n^2)n^2} \leqslant \frac{Re^3}{8}\sum_{n=1}^{\sqrt{N}}\frac{1}{N^2+n^4}$$

$$\leqslant \frac{Re^3}{8N^2}\sum_{n=1}^{\sqrt{N}}\frac{1}{1+(n/\sqrt{N})^4} \leqslant \frac{Re^3}{8N^2}\sum_{n=1}^{\sqrt{N}}1 = \frac{Re^3}{8N^{1.5}}.$$

Therefore neglecting asymptotically smaller terms we have

$$\frac{1}{Re}\langle \partial\chi^-_{upper} \cdot \boldsymbol{S}\partial\chi^-_{upper}\rangle = -\langle \partial(\chi^+_{upper}+e)\cdot \boldsymbol{H}\partial\chi^-_{upper}\rangle \leqslant \frac{Re^3}{96N}. \tag{A 42}$$

We also have with (A 30*a*, *c*)

$$\frac{1}{Re}\langle \partial\chi^+_{upper} \cdot \boldsymbol{S}\partial\chi^+_{upper}\rangle \leqslant 2Re\sum_{m,n\geqslant 0, m*n<N}(n^2+m^2)\langle \cos(2n+1)y_1 \cos(2m+1)y_2\rangle$$

$$\leqslant \frac{Re}{2}\sum_{m,n>0, m*n<N}(n^2+m^2) \leqslant 2\frac{Re}{2}\sum_{n=1}^{N} n^2\frac{N}{n} \leqslant \frac{Re}{2}N^3. \tag{A 43}$$

Combining (A 42) and (A 43) for any N

$$U(\chi^+_{upper}, \chi^-_{upper}, e) \leqslant \frac{Re^3}{96N} + \frac{Re}{2}N^3.$$

Choosing the optimal

$$N = \frac{\sqrt{Re}}{48^{1/4}}$$

we have

$$\frac{v'}{2} \leqslant 48^{-3/4}Re^{2.5}. \tag{A 44}$$

□

REFERENCES

Bensoussan, A., Lions, J. & Papanicolaou, G. 1978 *Asymptotic Analysis for Periodic Structures.* North-Holland.

Cherkaev, A. & Gibiansky, L. 1994 Variational principles for complex conductivity, viscoelasticity, and similar problems in media with complex moduli. *J. Math. Phys.* **35**, 127–145.

Cushman-Roisin, B. 1994 *Introduction to Geophysical Fluid Dynamics.* Prentice-Hall.

https://doi.org/10.1017/S0022112001005730 Published online by Cambridge University Press

Cushman-Roisin, B., McLaughlin, D. & Papanicolaou, G. 1984 Interactions between mean flow and finite-amplitude mesoscale eddies in a barotropic ocean. *Geophys. Astrophys. Fluid Dyn.* **29**, 333–353.

Dubrulle, B. & Frisch, U. 1991 Eddy viscosity of parity-invariant flows. *Phys. Rev.* A **43**, 5355–5364.

Fannjiang, A. & Papanicolaou, G. 1994 Convection enhanced diffusion for periodic flows. *SIAM J. Appl. Maths* **54**, 333–408.

Fannjiang, A. & Papanicolaou, G. 1997 Convection enhanced diffusion for random flows. *J. Statist. Phys.* **88**, 1033–1076.

Frisch, U., She, Z. & Sulem, P. 1987 Large-scale flow driven by the anisotropic kinetic alpha effect. *Physica* D **28**, 382–392.

Gama, S., Vergassola, M. & Frisch, U. 1994 Negative eddy viscosity in isotropically forced two-dimensional flow: linear and nonlinear dynamics. *J. Fluid Mech.* **260**, 95–126.

Gelfand, I. & Fomin, S. 1963 *Calculus of Variations.* Prentice-Hall.

Isichenko, M. 1992 Percolation, statistical topography, and transport in random media. *Rev. Mod. Phys.* **64**, 961–1043.

Kraichnan, R. 1976 Eddy viscosity in two and three dimensions. *J. Atmos. Sci.* **33**, 1521–1536.

Meshalkin, L. & Sinai, Y. 1961 Investigation of the stability of a stationary solution of a system of equations for the plane movement of an incompressible viscous liquid. *Appl. Math. Mech.* **24**, 1700–1705.

Milton, G. 1990 On characterizing the set of possible effective tensors of composites: the variational method and the translational method. *Commun. Pure Appl. Maths* **43**, 63–125.

Mohammadi, B. & Pironneau, O. 1994 *Analysis of the k-epsilon Model.* Wiley.

Moiseev, S., Rutkevich, A., Tur, A. & Yanovskii, V. 1984 Vortex dynamo in a convective medium with helical turbulence. *Sov. Phys. JETP* **67**(2), 294–299.

Monin, A. & Ozmidov, R. 1985 *Turbulence in Oceans.* Dordrecht.

Nepomnyashchy, A. 1976 On the stability of the secondary flow of a viscous fluid in an infinite domain. *Appl. Math. Mech.* **40**, 886–891.

Rüdiger, G. 1989 *Differential Rotation and Stellar Convection.* Akademie-Verlag.

Sivashinsky, G. 1985 Weak turbulence in periodic flows. *Physica* D **17**, 243–255.

Sivashinsky, G. & Frenkel, A. 1992 On negative eddy viscosity under conditions of isotropy. *Phys. Fluids* A **4**, 1608–1610.

Sivashinsky, G. & Yakhot, V. 1985 Negative viscosity effect in large-scale flows. *Phys. Fluids* **28**, 1040–1042.

Starr, V. 1968 *Physics of Negative Viscosity Phenomena.* McGraw-Hill.

Sulem, P., She, Z., Scholl, H. & Frisch, U. 1989 Generation of large-scale structures in three-dimensional flow lacking parity-invariance. *J. Fluid Mech.* **205**, 341–358.

Wirth, A., Gama, S. & Frisch, U. 1995 Eddy viscosity of three-dimensional flow. *J. Fluid Mech.* **288**, 249–264.

https://doi.org/10.1017/S0022112001005730 Published online by Cambridge University Press